Usefulness of Non-Uniform Heating and Quenching Method for Residual Stress of Bimetallic Roll: FEM Simulation Considering Creep Behavior

DOI: 10.1002/srin.201600165
Article type: Full Paper

Usefulness of Non-Uniform Heating and Quenching Method for Residual Stress of Bimetallic Roll: FEM Simulation Considering Creep Behavior

N.-A. NODA*, K. J. HU, Y. SANO, K. ONO and Y. HOSOKAWA

Department of Mechanical Engineering, Kyushu Institute of Technology,
1-1 Sensui- cho, Tobata-ku, Kitakyushu-shi, Fukuoka, 804-8550 Japan
E-mail: noda@mech.kyutech.ac.jp

Keywords: residual stress, work roll, quenching, FEM, creep

Bimetallic rolls are widely used in steel rolling industries because of the excellent hardness, wear resistance and high temperature properties. Controlling the residual stress distribution is important to improve the roll fatigue life due to the compressive residual stress at the roll surface. Recently, to reduce the tensile residual stress appearing at the roll center, quenching heat treatment is performed just after heating the roll non-uniformly instead of heating the roll uniformly with enough time. In this paper, therefore, the residual stresses are compared after between the uniform heating quenching and the non-uniform heating quenching on the basis of the FEM simulation. The results show that tensile stresses at the roll center for non-uniform heating are smaller than that for uniform heating by 400MPa although the same compressive stresses appear at the surface. The effect of creep on stress relaxation is also considered in this study. By considering creep, the maximum tensile residual stress decreases by 8% for uniform heating and by 15% for non-uniform heating.

1. Introduction

The bimetallic rolls are widely used at the roughing stands of hot strip rolling mills, which must meet excellent hardness, wear resistance at the surface and high strength, high toughness at the center.[1-3] Bimetallic roll is manufactured by centrifugal casting method, using high speed steel (HSS) as shell material and the ductile casting iron (DCI) as core material. During

hot rolling process, thermal stresses are caused by a cyclic sequence of heating – cooling over the roll surface due to hot strip contact and water cooling,[4-7] resulting in thermal crack initiation named firecrack at the roll surface. If severe thermal tensile stress has been added under the rolling trouble, the thermal crack starts to propagate. Therefore, suitable compressive stresses are necessary for preventing the thermal crack extension.[8] However, the tensile residual stress always appears at the roll center to balance the surface compressive residual stress. Under the combined action of thermal stress and residual stress, another form of roll fracture is known as thermal barrel breakage. This thermal breakage was originating near to the roll center and breaking out to the barrel surface.[9-11] The residual tensile stress affects the thermal breakage because if the total tensile stress exceeds the strength of core material, a sudden thermal breakage happens. Decreasing the center tensile stress is therefore desirable to reduce the risk of fracture from the roll center. Since the residual stress can be controlled by the heat treatment, an appropriate quenching process has been required to improve bimetallic roll quality.

Although previous studies treated the quenching process for HSS bimetallic roll, they mainly focused on the quenching temperature affecting the microstructure and mechanical properties of material.[12-14] For example, the previous experimental results shows that the hardness of HSS roll increases with increasing the quenching temperature and the hardness decreases when the temperature exceeds 1040℃. However, no detail studies are available for the effect of quenching process on the residual stress. Therefore, in our previous study, the residual stress simulation was performed for quenching of bimetallic rolls after the roll was heated up uniformly.[15] Then, the generation mechanism and distribution of residual stress were investigated. Also, the effects of the shell-core ratio, diameter, phase transformation and material heat treatment process on the residual stress were discussed. However, the effects of creep behavior and thermal stress on residual stress of bimetallic rolls have not yet been considered in the previous study.

In this paper, the simulation will be performed for quenching after non-uniform heating, which is a different quenching method recently developed and widely used for bimetallic rolls.[16-18] Although the previous studies referred the residual stress due to this quenching after non-uniform heating,[19] the detail effect on the residual stress generation has not been discussed yet. Therefore, in this study, the usefulness of this method for the residual stress will be investigated for bimetallic rolls. The stress relaxation caused by creep behavior will be also considered. Then, the results will be compared with the results of quenching after uniform heating. The effect of non-uniform heating on the residual stress of HSS bimetallic roll will be clarified through the comparison. The results will be useful for determining an appropriate quenching process of HSS bimetallic rolls.

2. Quenching after non-uniform heating and FEM modeling

Figure 1(a) illustrates the non-uniform heating quenching process in comparison with **Figure 1(b)**, which illustrates the uniform heating quenching process. In the uniform heating process, the whole roll is heated up to the higher temperature equaling to T_{Start} before the quenching process. In the non-uniform heating process, the whole roll is heated up to the uniform lower temperature of T_{Heat} and kept at T_{Heat} for some hours, then rapidly heated up to T_{Start} as the non-uniform heating before quenching. This rapid heating provides temperature difference between the roll surface and roll center. The quenching processes after non-uniform heating and uniform heating are similar, but the keeping temperature T_{Keep1}in Figure 1(a) $>$ T_{Keep2} in Figure 1(b). The quenching process after the non-uniform heating quenching can be described in the following way.

The roll is put out from the heating furnace and cooled down rapidly from T_{Start} by using the spray cooling. After rapid cooling, the roll is maintained for several hours when the surface temperature drops to T_{Keep1}. Here, keeping T_{Keep1} is beneficial to relaxing the excessive

thermal stresses caused by rapid surface cooling. After keeping T_{Keep1}, the roll is put out from the furnace and slowly cooled down in air until to T_{Finish}. Since the tempering process has not been performed, these residual stresses just after quenching process are called middle residual stresses. After quenching process, usually the tempering process will be performed 2 to 4 times to release the residual stress and obtained the stable microstructure. The effect of tempering process will not be considered in this study and will be studied in the future.

As shown in **Figure 2(a)**, the roll diameter is 660mm, body length is 1600mm and shell thickness is 60mm, consisting of the high speed steel as shell and the ductile casting iron as core and roll neck. **Table 1(a)** shows the chemical compositions of high speed steel and ductile casting iron for the common HSS bimetallic rolls,[20] and **Table 1(b)** shows the material properties of high speed steel and ductile casting iron at room temperature.

Figure 2(b) shows the FEM mesh and boundary conditions to simulate the non-uniform heating and quenching. MSC.Marc 2012 software is used for elastic-plastic analysis to simulate the quenching process for HSS bimetallic rolls. The roll clutch with the length of 400mm is ignored because of the small effect on the residual stress at the central section. A 4-node linear axisymmetric quad element with the mesh size of 5×5mm is adopted for the transient-static simulation. The displacement boundary conditions and thermal isolation conditions are applied to z=0 due to the symmetry. In this study, roll surface temperature $T_{surface}$ measured experimentally is imposed to the roll surface. A large amount of material properties of the shell and core materials were measured from T_{Start} to T_{Finish} at a certain interval of temperature and used in the simulation as input data. Those material properties include Young's modulus, thermal expansion coefficient, specific heat, thermal diffusion, density, yield point, thermal conductivity and Poisson's ratio. During the quenching process, the pearlite transformation occurs in the core material and bainite transformation occurs in the shell material. Volume expansions of core and shell accompany the phase transformations. Similar to the previous study,[15] the thermal expansion coefficients are used as input data to

express the volume expansions.

3. Summary of residual stress due to uniform heating quenching

In the previous study,[15] the residual stress was discussed for the quenching process after conventional uniform heating. To discuss the effects of non-uniform heating quenching, the results of the uniform heating quenching should be summarized. Figure 3 shows (a) temperature histories and (b) stress σ_z histories at the surface and center under uniform heating quenching process. The residual stresses for the uniform heating quenching process can be summarized in the following way for heating process Ⓐ and quenching process ⒷⒸ ⒹⒺ.

In the heating processⒶ, the whole roll is slowly heated up to uniform temperature of T_{Start} in Figure 3. The stress does not appear since the temperature gradient is small enough between the surface and center during the heating process.

In the processⒷ at the beginning of the cooling, the tensile stress appears at the surface due to rapid surface cooling. Then, the center thermal contraction becomes larger than that at the surface, leading to the center stress changes from compression to tension. As a result, tensile stress at the surface reaches peak values then turn to opposite direction. As center temperature dropping to the temperature $T_{Pearlite}$ in Figure 3, pearlite transformation (expansion) happens near the shell/core boundary at time $t_1$and expands toward the center (see ⓟ from t_1 to t_3 in Figure 3(b)). In this period, the center is shrunk relative to the other parts of the core which expanded gradually due to pearlite transformation. Hence, the compressive stress at the center decreases until becomes tensile stress.

In the processⒸ, the tensile stress reverses to compressive stress rapidly when the pearlite transformation reaches to the center. After the pearlite transformation, the compressive stress

at the center decreases until becomes tensile stress due to the larger temperature change at the center(see ⓣ from t_3 to t_4 in Figure 3(b)). Then, the surface stress state interchanges from tension to compression, and the center stress state interchanges from compression to tension. These stress states are kept until the end of keeping process.

In the process Ⓓ, at the beginning of T_{Keep2}, both stresses at the center and surface increase due to the roll is transferred into holding furnace and the surface temperature slightly increases. After surface temperature reaching the stable temperature of T_{keep2} in Figure 3, the stresses at the surface and the center decrease gradually because of the decreasing of temperature gradient.

In the process Ⓔ, bainite transformation occurs at the surface, causing a volume expansion and the surface compressive stress increasing. To balance the increase of surface stress, the center tensile stress also increases. After the bainite phase transformation, the thermal contraction difference becomes larger and Young's modulus increases with decreasing temperature. Eventually, both surface and center residual stresses increase continuously.

Figure 3(c) shows the residual stress distributions of the component σ_z, σ_r, σ_θ and Mises stress σ_{eq} after uniform heating quenching. It is seen that the tensile stress σ_z=388MPa is much larger than the stress σ_{eq}=269MPa at the roll center, and other stresses σ_θ, σ_r are much smaller around the center. The maximum stress σ_z = 388MPa is close to the tensile strength 415 MPa indicated in Table 1(b) and risky for roll thermal barrel breakage if thermal tensile stress is added during hot rolling process.

4. Residual stress due to non-uniform heating quenching

4.1 Residual stress generation during quenching after non-uniform heating

Figure 4 shows (a) temperature histories and (b) stress σ_z histories at the surface and center under non-uniform heating quenching process. The residual stress during non-uniform heating quenching process can be explained in the following way.

In the process Ⓐ of non-uniform heating, the whole roll is heated up to T_{Heat} and kept at T_{Heat} for several hours. After that, as shown in Figure 4(a), the roll is rapidly heated up before the roll surface temperature reaches T_{Start}. During this rapid heating process, the surface temperature rises faster than the center temperature, causing the compressive stress at the surface and causing the tensile stress at the center. When surface temperature is heated up to the temperature $T_{Austenite}$ in Figure 4(a), the austenite transformation occurs at the surface. The volume shrinkage due to the austenite transformation leads to the compressive stress decreases until becomes tensile stress at the surface as shown in ⓐ in Figure 4(b). However, since the austenite transformation extends toward the shell-core boundary, the tensile stress at the surface becomes compressive stress immediately. After austenite transformation, since the temperature difference between the surface and core becomes smaller, the compressive stress at the surface decreases and the tensile stress at the center also decrease.

In the processes Ⓑ Ⓒ, due to the rapid cooling of surface temperature, the larger peak tensile stress appears at the roll surface (see ⓑ in Figure 4(b)). Similarly to the pearlite transformation during uniform heating quenching (see ⓟ in Figure 3(b)), the compressive stress at the center firstly decreases and then increases (see ⓟ from t_1 to t_3 in Figure 4(b)). However, the center stress is always in compression during pearlite transformation. After the pearlite transformation, the compressive stress at the center decreases slightly (see ⓣ from t_3 to t_4 in Figure 4(b)).

In the process Ⓓ the roll is transferred into holding furnace resulting in surface temperature rising. As a result, surface stress moves from tension to compression. To balance the surface stress, the center compressive stress decreases. The temperature gradient decreases gradually

during the keeping process at T_{Keep1}, and both of tensile stress and compressive stress are slightly changed.

In the process Ⓔ, after the keeping period at T_{Keep1}, the roll is transferred out holding furnace and cooled in air. The surface temperature is dropped fast, causing temperature gradient increasing. As a result, compressive stress at the center decreases until becomes to tensile stress, and compressive stress at the surface increases. Similar to the bainite transformation during uniform heating quenching, volume expansion occurs at roll surface and the stress reverses from tension to compression. Meanwhile, the center compressive stress decreases to balance the surface stress.

Figure 4(c) shows the residual stress distributions of the components σ_z, σ_r, σ_θ, σ_{eq} after non-uniform heating quenching. All stress components σ_z, σ_r, σ_θ are compressive at the center. The maximum tensile stress σ_z=216MPa at r=200mm in Figure 4(c) is much smaller than the maximum σ_z =388MPa at the roll center in Figure 3(c). Those residual stress distributions are useful for reducing the risk of fracture. Since σ_z is larger than other stress components, σ_z will be mainly discussed in the following sections.

4. 2 Residual stress generation mechanism after non-uniform heating quenching

Figure 5 shows stress distributions σ_z along the central cross section where z=0. It is seen that the residual stress distributions are quite different depending on the non-uniform and uniform heating methods. The maximum tensile stress of the non-uniform heating appears near the shell/core boundary since the center stress decreases by (388) - (-58) = 446MPa compared with the one of uniform heating. Although the surface compressive stress is smaller for the non-uniform heating quenching, the value looks large enough to prevent the thermal crack. The results show that the non-uniform heating quenching is useful for reducing the risk of roll

fracture by providing sufficient compressive stresses at the roll surface as well as smaller tensile stresses at the roll center.

In this paper, as shown in Figure 6 and Figure 7, two aspects will be focused in order to explain why the center stress can be reduced in non-uniform heating quenching. One is the pearlite transformation effect in ⓟ and temperature effect in ⓣ before keeping T_{Keep1} and T_{Keep2}(see Figure 6), and the other is the cooling effect after keeping T_{Keep1} and T_{Keep2} (see Figure 7).

Figure 6 shows the residual stress distributions σ_z during the period Ⓑ and Ⓒ at $t_1 \sim t_4$ indicated in Figure 3 and Figure 4. Here , t_1 is the beginning time of pearlite transformation at shell/core boundary, t_2 is the beginning time of pearlite transformation at roll center, t_3 is the ending time of pearlite transformation at the roll center, t_4 is the beginning time of keeping process.

At t_1, the tensile stress appears at shell and compressive stress appears at core after the rapid cooling for two kinds of quenching. Since the higher surface cooling speed in non-uniform heating quenching, the tensile stress and compressive stress is larger than that in uniform heating quenching.

At t_2, the pearlite transformation occurs at shell/core boundary, therefore, the compressive stresses near to the boundary increase and the compressive stresses near to the center decrease. From t_1 to t_2, the center stress change is (-106) - (-157) = 51MPa in non-uniform heating quenching and it change is (80) - (-108) = 188MPa in uniform heating quenching. The center compressive stress change is much smaller in non-uniform heating quenching compared with the stress in uniform heating quenching. This is because the center cooling speed in non-uniform heating quenching is lower than that in uniform heating quenching.

At t_3, the pearlite transformation occurs at center, therefore, the center compressive stresses increase. From t_2 to t_3, the center stress change is (-253) - (-106) = -147MPa in non-uniform

heating quenching and it changes (-78) - (80) = -158MPa in uniform heating quenching. The center compressive stress changes are very close from t_2 to t_3.

From t_3 to t_4, the center stress change is (-232) - (-253) = 21MPa in non-uniform heating quenching and the change is (130) - (-78) = 208MPa in uniform heating quenching. The center compressive stress change is much smaller in non-uniform heating quenching compared with the change in uniform heating quenching. This is also because the center cooling speed in non-uniform heating quenching is lower than that in uniform heating quenching. It may be concluded that the center stress for non-uniform heating quenching increases slightly before and after pearlite transformation and causing the smaller residual stress at the center.

Figure 7 shows the stress distribution σ_z at the central cross section where z=0 after bainite transformation when the surface temperature is 400℃, 300℃ and 200℃. In the case of uniform heating quenching, the core stress distribution shifts to the tension side with decreasing the temperature without changing the distribution shape. In a similar way, the shell stress distribution shifts to the compressive side with decreasing the temperature without changing the distribution shape. The stress gap at the shell-core boundary becomes smaller with decreasing the temperature. In the case of non-uniform quenching, the stress distributions shift without changing the distribution shape in a similar way. Moreover, the center stress change is (336) - (138) = 198MPa and surface stress change is (-435) - (-13) = -422MPa in surface temperature ranges from 400℃ to 200℃ for uniform heating quenching. Similarly, the center stress change is (-94) - (-281) = 197MPa and surface stress change is (-353) - (76) = -429MPa for non-uniform heating quenching. The amounts of center compressive stress changes are very close. It may be concluded that the final shape of stress distribution is mainly depending on the cooling process before keeping temperature T_{Keep1}.

4.3 Roll center fracture named thermal barrel breakage may be prevented by non-uniform heating quenching

During the hot rolling process, the roll surface temperature becomes 800℃ due to the contact of hot rolled material, then the roll is rapidly cooled down by water cooling. This repeated temperature changes may cause thermal fatigue cracks at the roll surface. On the other hand, thermal barrel breakage may occur at the beginning of the rolling. This thermal barrel breakage is related to the maximum temperature difference between the roll center and sub-surface. This temperature difference initiates thermal stresses which are superimposed on the existing residual stresses in the roll. In Ref[11], A temperature difference 70°C causes additional thermal stresses about 110Mpa.

It is known that the roll temperature distribution has a sharp thermal gradient near to the roll surface because of the existence of thermal skin layer.[6, 21] The depth of the thermal skin layer can be estimated about only 1% of the radius. For this reason, the temperature of sub-surface about 1mm below the surface beyond the thermal skin layer should be considered as the base surface temperature. The temperature distribution between the sub-surface and the center can be approximated by the linear distribution as shown in reference.[6] It was confirmed that a linear temperature distribution provides the larger stress at the roll center compared with the real thermal stress. In other words, a linear temperature distribution between the sub-surface and center can be used to evaluate the thermal stress safely. At the initial hot rolling process the maximum temperature difference has been reported as the sub-surface temperature is 70℃ [22] and the roll center temperature is 40℃[21]. To verify the usefulness of non-uniform heating and quenching method, those data will be applied to the thermal stress analysis in this study.

In Figure 5 the thermal stress caused by temperature difference is also indicated as the dashed line. The thermal stress is calculated by using the FEM simulation. The FEM model is the

same as the bimetallic roll as shown in Figure 2(b). The linear temperature distribution between the sub-surface and center is applied to the model. The required material properties including Young's modulus E(E_{HSS} and E_{DCI}), thermal expansion coefficient α(α_{HSS}, α_{DCI})and Poisson's ratio ν (ν_{HSS}, ν_{DCI}) are given as Table 1(b). Since the residual stresses at the core has a higher fracture risk than the shell, the thermal stress is considered to be added to the existing residual stress at the core.

As shown in Figure 5, in the uniform heating quenching, the maximum stress σ_z becomes 388+43=431MPa at the roll center by combining the residual and thermal stresses. In the non-uniform heating quenching, the combined stress σ_z is (-58)+43= -15MPa at the roll center and the maximum stress σ_z is 216+(-6)=210MPa near the boundary.

To discuss the risk of the roll center fracture, the safety factor is defined as σ_B/σ_z from the tensile strength σ_B and the axial stress σ_z. In the non-uniform heating quenching, we have $|\boldsymbol{\sigma_B} / \boldsymbol{\sigma_z^{center}}|$=27.67 at the roll center and $\sigma_B/\boldsymbol{\sigma_z^{interface}}$=1.98 near the boundary. They are quite larger and therefore safer than the value $\sigma_B/\boldsymbol{\sigma_z^{center}}$=1.04 in the uniform heating quenching.

To ensure the safety, it is empirically known that the safety factor $\sigma_B/\sigma_z \geq 1.2$ is required in the roll design. In the uniform heating quenching, the value $\sigma_B/\boldsymbol{\sigma_z^{center}}$=1.04 is much smaller than the required safety factor $\sigma_B/\sigma_z \geq 1.2$. On the other hand, in the non-uniform heating, the safety factor $\sigma_B/\boldsymbol{\sigma_z^{interface}}$=1.98 at the most dangerous point is larger enough than the required safety factor $\sigma_B/\sigma_z \geq 1.2$. Therefore, it may be concluded that the roll safety can be significantly improved by using non-uniform heating quenching method.

In the above thermal stress analysis, the assumed residual stress was obtained from the analysis just after quenching process. However, it is known that the actual residual stress may decrease by 30% through the tempering process repeated 2-4 times. Assuming by 30% reduction in the uniform heating quenching, the center residual stress σ_z becomes 272MPa due to

the tempering. Then, we have $\sigma_B/\boldsymbol{\sigma_z^{center}}$=1.32 satisfying the safety condition $\sigma_B/\sigma_z \geq 1.2$. Therefore, the roll safety is also assured in uniform heating quenching under the roll cooling system without troubles. It may be concluded that the roll safety is guaranteed more easily in the non-uniform heating quenching than in the uniform heating quenching.

5. Usefulness of quenching after non-uniform heating

As shown in the above discussion, it is found that the non-uniform heating quenching is useful for reducing the risk of roll failure by decreasing the center tensile stress. Generally, the usefulness of non-uniform heating quenching can be summarized in the following way.

① The pre-heating time is shortened by using non-uniform heating method, which contributes to energy saving.

② The quenching time is also shortened as well as pre-heating time by using the non-uniform heating quenching, which contributes to shorten the operation time of high temperature.

③ The quenching temperature of the core material is lower than 900℃, which contributes to prevent material deterioration induced by excessive heating.

④ As shown in the above discussions, the non-uniform heating quenching is useful for reducing the risk of failure by decreasing the center tensile stress without decreasing the surface compressive stress.

⑤ The material microstructure can be fined and a few martensitic structures can be produced due to the rapid cooling rate of quenching. As a result, a hard shell is obtained to improve the impact strength and strength of roll during the hot rolling.

6. Effect of creep behavior on residual stress

In this study, the usefulness of the quenching after non-uniform heating was discussed on the bases of FEM simulation considering creep behavior. In this chapter, the creep analysis and the effect on the residual stress will be explained. Creep can be defined as a time-dependent deformation at elevated temperature under a constant stress. Stress relaxation can be defined as a decrease in stress under constant strain. Those two are closely associated important phenomena which should be considered in the design of engineering components. The finite element analysis requires that stress relaxation be modeled using creep equations.

6.1 Creep analysis

In Figure 3 and Figure 4, the creep effect looks small in the region Ⓑ Ⓒ because the temperature changes quite largely as well as the stress. Also, in the region Ⓔ the creep effect looks small because of the lower temperature. Therefore, the creep analysis is applied to the keeping process Ⓓ where the roll is put at relatively high temperature for several hours.

In the creep analysis, the transient creep strain also should be considered as well as the steady creep strain. Among several equations available for creep analyses, the time hardening law, sometimes called power law, is used to express the core material which has low strength under high temperature. It should be noted that the creep should be considered in a short hours Ⓓ for the roll quenching compared to the common creep analysis. The core creep can be given as **Equation (1)**.

$$\boldsymbol{\varepsilon_c = A\sigma^m t^n} \tag{1}$$

where $\boldsymbol{\varepsilon_c}$is the transient strain, $\boldsymbol{\sigma}$ is stress, t is time, A, m and n are temperature dependent material constants. This time hardening formulation is used to predict the creep behavior

under a variable stress history. In order to determine constants A, m and n, the creep tests are performed.

6.2 Creep and stress relaxation test

6.2.1 Creep test

The creep testing was conducted by using a miniature creep rupture testing machine based on JISZ2271.[23] The specimens were prepared from core material as shown in **Figure 8(a)**. Those specimens were respectively heated up to the testing temperatures, T_{keep1} and T_{keep2}, and kept at theses temperatures during the testing process. Then, the creep tests were carried out by applying constant loads 100MPa and 130MPa. The strain changes were recorded with time. From the strain-time curves obtained, the creep equations can be written as shown in **Equations (2) and (3)**.

$$\boldsymbol{\varepsilon_c = 2.25\times10^{-13}\sigma^{3.44}t^{0.672}} \ (T_{keep1}) \tag{2}$$

$$\boldsymbol{\varepsilon_c = 8.38\times10^{-19}\sigma^{5.71}t^{0.514}} \ (T_{keep2}) \tag{3}$$

6.2.2 Stress relaxation test

To confirm the validity of Equations (2) and (3), the following stress relaxation testing was conducted. The specimens were prepared from the core material as shown in **Figure 8(b)**. Those specimens were respectively heated up to the testing temperature, T_{Keep1} and T_{Keep2}, and kept at theses temperatures during the testing process. Then, the stress relaxation tests were carried out under the constant strain when the primary stress is 130MPa. The time and stress changes were recorded as shown in Figure 9.

6.3 Results and discussion for creep

The FEM simulation of stress relaxation is performed to verify Equations (2), (3) in **Figure 9** in comparison with the experimental result at T_{Keep1} and T_{Keep2}. The results show that the stress decreases by 69% at Tkeep1 and by 38% at T_{keep2}. It can be found that the stress relaxation ratio is larger at high temperature (T_{Keep1}) than relatively low temperature (T_{Keep2}). The FEM results are in good agreement with the experiment results. It is confirmed that Equations (2), (3) are useful for predicting the creep effect on the residual stress.

6.4 Effect of creep behavior on residual stress

Figure 10 shows stress distribution σ_z along the central cross section where z=0 with and without considering creep. For non-uniform heating quenching, the maximum stress at the core decreases by 15% from 216MPa to 185MPa and the center stress decreases from -58 MPa to -33 MPa by considering creep. For uniform heating quenching, the center stress decreases by 8% form 388MPa to 357MPa by considering creep. The stresses become uniformly distributed at the core no matter which quenching process (uniform or non-uniform) is considered during heating. However, the surface stresses are almost unchanged by considering creep in both quenching processes.

Table 2 compares the keeping process between non-uniform heating quenching and uniform heating quenching including the stress relaxation ratio, keeping temperature, Mises stress σ_{eq} and keeping time. The non-uniform heating quenching has larger stress relaxation and larger Mises stress than uniform heating quenching. Among of these factors, the stress relaxation plays a dominant role on the final stress decrease. Because of this reason, as shown in Figure 10, the creep effect for non-uniform heating quenching becomes larger than that for uniform heating quenching.

7. Conclusions

In this paper, FEM simulation of non-uniform heating quenching for bimetallic roll was performed to predict the residual stress distribution. The residual stresses were compared between uniform heating quenching and non-uniform heating quenching. Moreover, the creep effect on the residual stress has been discussed. The results of the current study can be summarized as follows.

(1) By using non-uniform heating quenching method, the maximum tensile stress in the core appears near the shell/core boundary, the center stress decreases by 446MPa and the maximum tensile stress decreases by 44% (see Figure 5). However, the compressive stress at the surface is almost unchanged. It may be concluded that non-uniform heating quenching is useful for reducing the risk of roll failure known as thermal barrel breakage by decreasing the center tensile stress without decreasing the surface compressive stress.

(2) The center stress increases slightly for non-uniform heating quenching before and after pearlite transformation and therefore the smaller residual stress appears at the center (see Figure 6). Then, the core stress distribution shifts to the tension side with decreasing the temperature without changing the distribution shape (see Figure 7). Similarly, the shell stress distribution shifts to the compressive side with decreasing the temperature without changing the distribution shape (see Figure 7).

(3) The thermal stress calculated by considering temperature difference between the sub-surface and the center is simulated and added to residual stress. It may be concluded that the roll safety is guaranteed more easily in the non-uniform heating quenching than in the uniform heating quenching (see Figure 5).

(4) The time hardening formulation calculated based on creep test data, is used to predict the effect of creep behavior on stress relaxation. The results show that the stress decreases by 69% at T_{keep1} and by 38% at T_{keep2} (see Figure 3(a) and Figure 4(a)).

(5) For non-uniform heating quenching, by considering creep, the maximum tensile stress at the core decreases by 15% from 216MPa to 185MPa and the center tensile stress decreases from -58 MPa to -33 Mpa (see Figure 10(a)). For uniform heating quenching, by considering creep, the center stress decreases by 8% form 388MPa to 357Mpa (see Figure 10(b)).

Received: ((will be filled in by the editorial staff))
Revised: ((will be filled in by the editorial staff))
Published online: ((will be filled in by the editorial staff))

[1] J. W. Choi and D. Kim, *ISIJ Int.* **1999**, *39* 823.

[2] H. Noguchi and Y. Watanabe, *Kawasaki Steel Giho*. **1987**, *19*, 195.

[3] M. Nilsson and M. Olsson, *Wear*. **2013**, *307*, 209.

[4] C. F. Onisa and D. C. J. Farrugia, *Int. J. Mate. Form.,* **2008**, *1*, 363.

[5] A. Pérez, R. L. Corral, R. Fuentes, and R. Colás, *J. Mater. Process. Technol.* **2004**, *153*, 894.

[6] D. Benasciutti, *J. Strain Analysis.* **2012**, *47*, 297.

[7] D. F. Chang, *J. Mater. Proc. Technol.* **1999***, 94*, 45.

[8] Y. Sano, T. Hattori and M. Haga, ISIJ Int. **1992**, *32*, 1194.

[9] Y. Sano and K. Kimura, *Tetsu-to-Hagane*. **1987**, 73, 1154.

[10] K. H. Schroder, *A basic understanding of the mechanics of rolling mill rolls*, Eisenwerk Sulzau-Werfen, ESW-Handbook, **2003**, 71.

[11] *Roll failures manual: Hot mill cast work rolls*, The European Foundry Association, Roll Section, **2002**, 19.

[12] H. G. Fu, A. M. Zhao and J. D. Xing, *J. Univ. Sci. Technol. Beijing*, **2003**, *10*, 62.

[13] H. G. Fu, H. J. Zhao, Z. Z. Du, Z. J. Feng, Y. P. Lei, Y. Zhang, M. W. Li, Y. H. Jiang, R. Zhou and H. X. Guo, *Ironmaking Steelmaking*. **2011**, *38*, 338.

[14] H. G. Fu, X. L Chen, Z. Z. Du, Y. P. Lei Zhenjun, *Journal China Foundr.* **2009**, *6*, 15.

[15] N.-A. Noda, K. Hu, Y. Sano, K. Ono and Y. Hosokawa, *Steel Research Int.* **2016**. DOI: 10.1002/srin.201500430.

[16] B. C. Liu, S. M. Zuo, *China Foundry Machinery & Technology*. **2015**, *4*, 18.

[17] C. P. Shen, *Heat Treat. Met.* **2003**, *28*, 50

[18] S. Li, C. J. Wu, J. X. SU and Y. J. Zhang, *J. Univ. Sci. Technol. Beijing*, **2010**, *32*, 331.

[19] J. Zhang and Z. P. Cheng, Sinosteel Xingtai Machinery& Mill Roll Co., Ltd. CN102352431 B, **2011**.

[20] N. Oda, Y. Nozaki, R. Honda and T. Ohata, Hitachi Metals, Ltd. WO2013042528 A1, **2013** (in Japanese).

[21] J. Kihara, Tetsu to Hagane, **1994**, 80, 386.

[22] S. Cerni, A. S. Weinstein and C. F. Zorowski, Iron and Steel Engineer. **1963**, *40*, 165.

[23] JISZ2271, Metallic materials-Uniaxial creep testing in tension-Method of test, Japanese Industrial Standards Committee, **2010**.

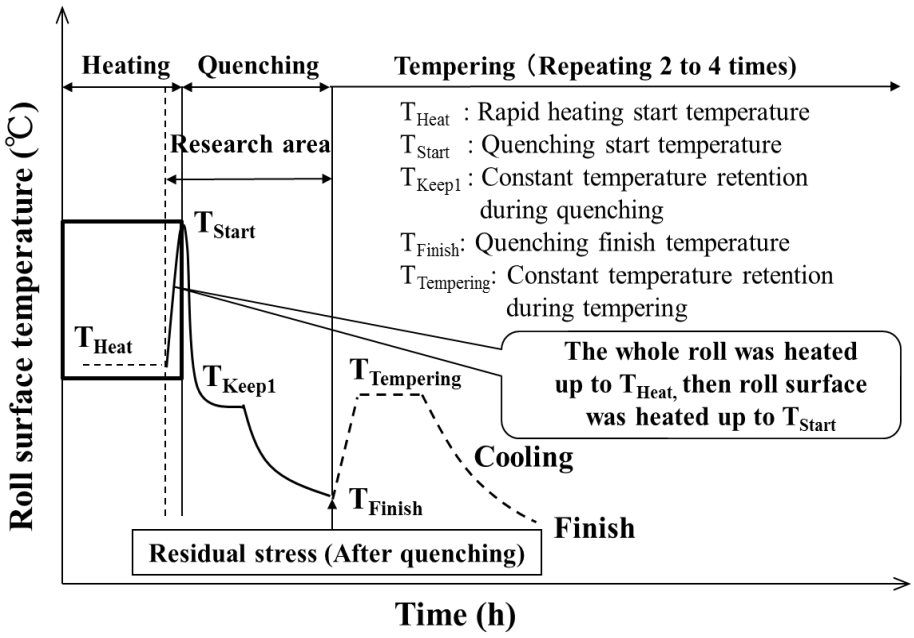

(a) Non-uniform heating and quenching process

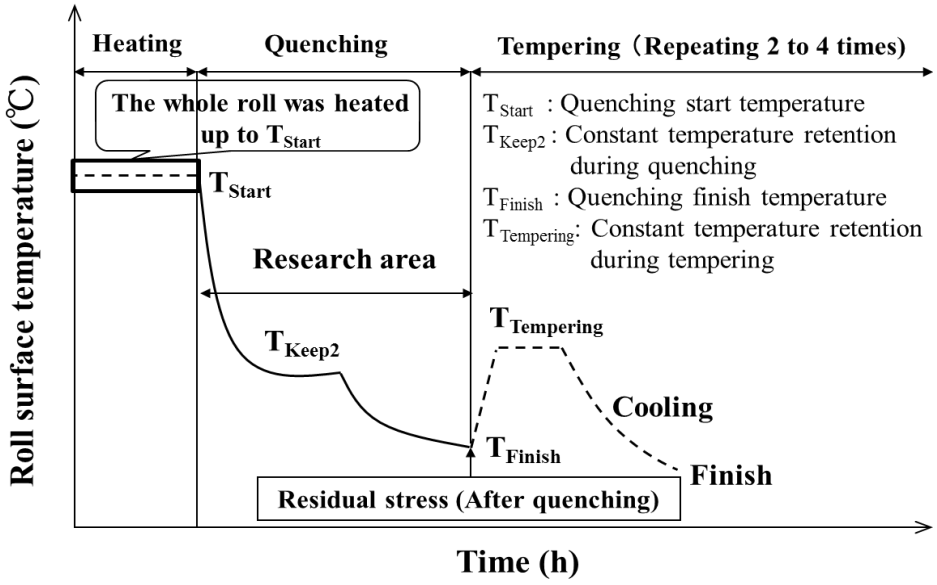

(b) Uniform heating and quenching process

Figure 1. Heating and quenching processes of HSS bimetalic roll

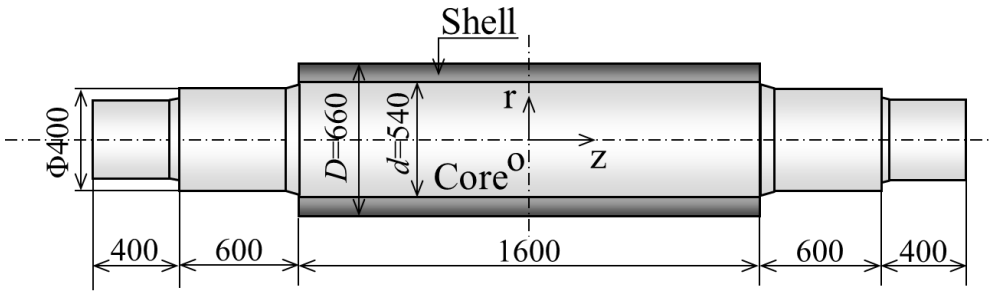

(a) Dimension of the HSS bimetallic roll (mm)

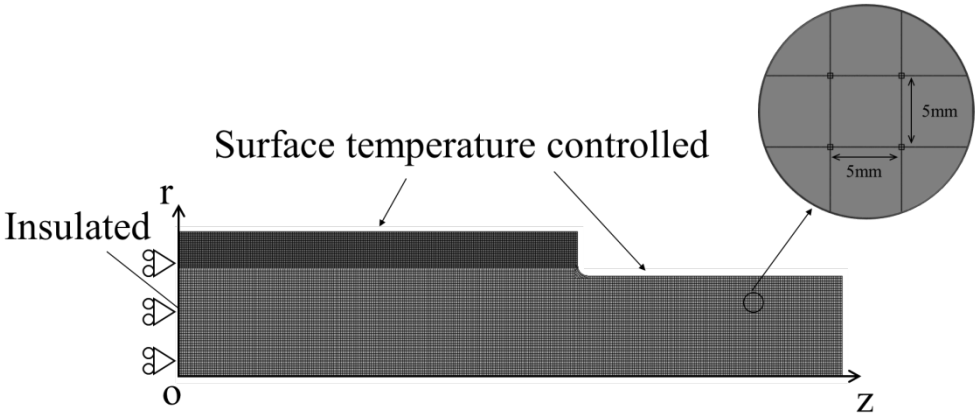

(b) FEM model and boundary conditions

Figure 2. FEM analysis of bimetallic roll

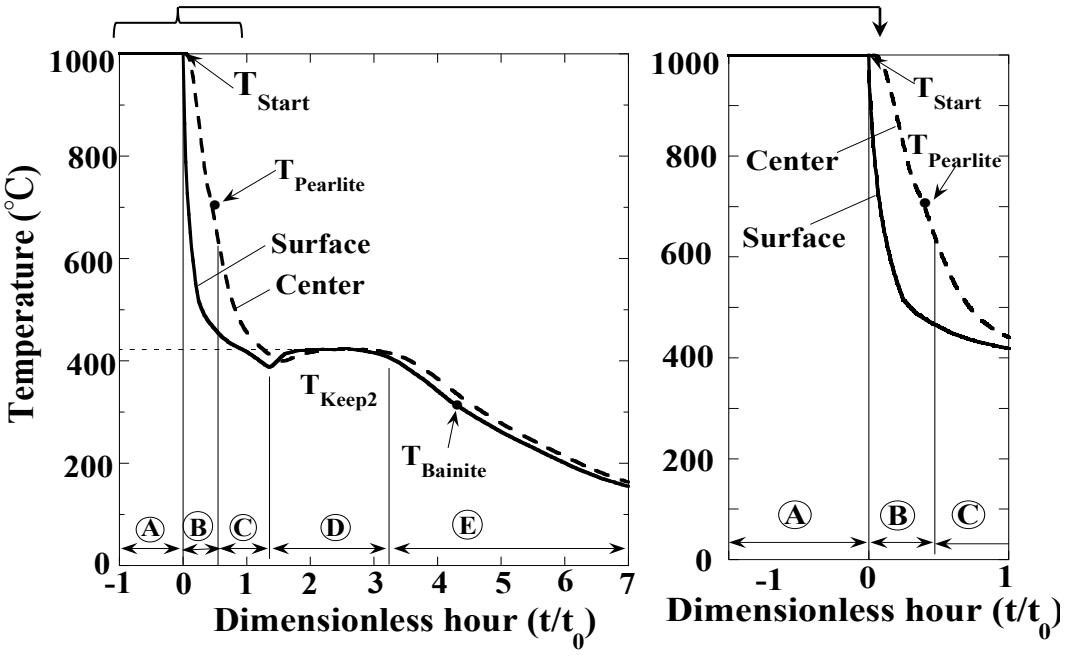

(a) Temperature histories at the center and surface

Ⓐ High-uniform temperature period
Ⓑ Rapid surface cooling period
Ⓒ Core material phase transformation period
Ⓓ Keeping temperature period
Ⓔ Furnace cooling and shell material phase transformation period

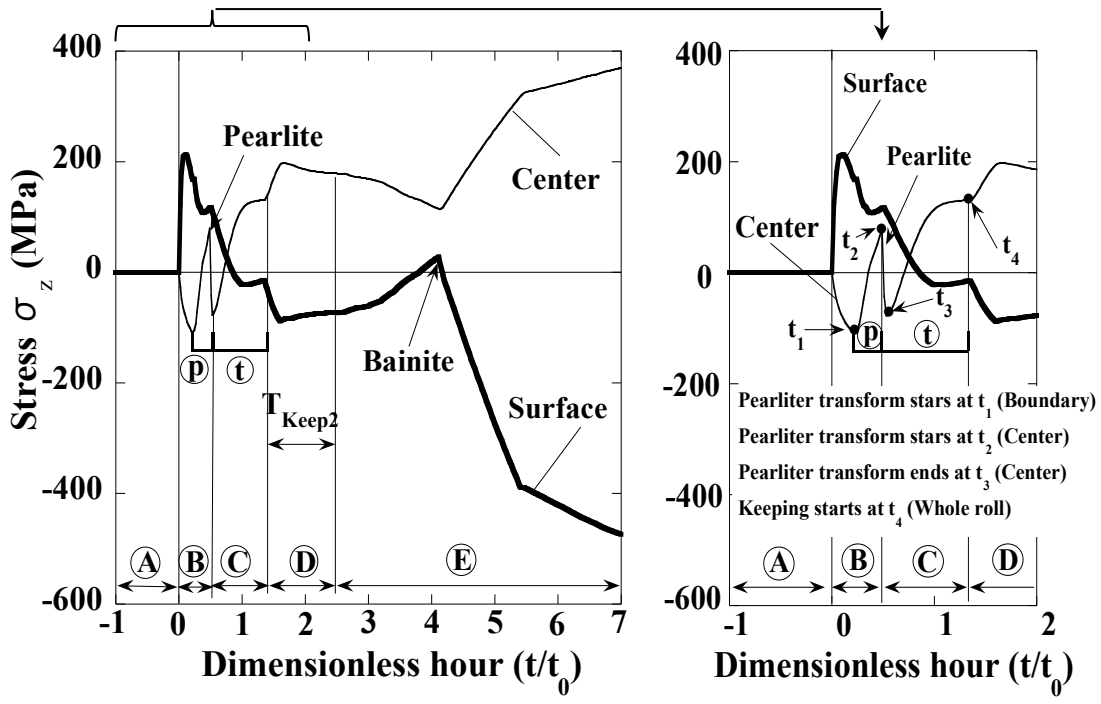

(b) Stress σ_z histories at center and surface

ⓟ Effect of pearlite transformation
ⓣ Effect of temperature decreasing

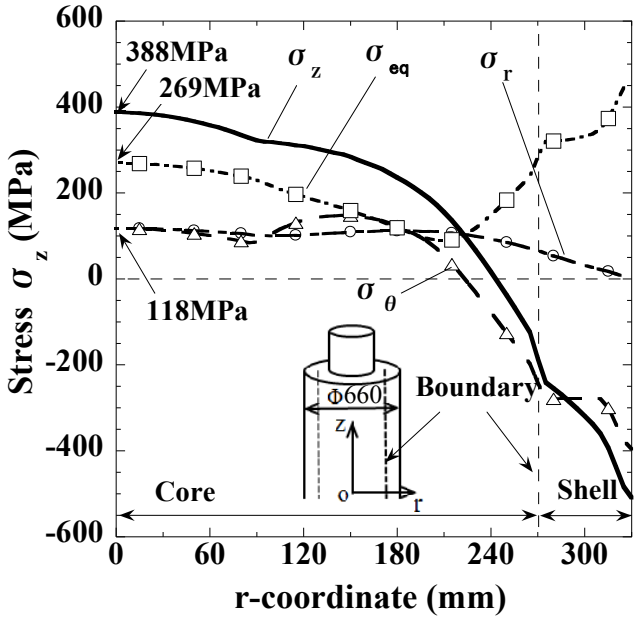

(c) Stress distribution from center to surface

Figure 3. Uniform heating quenching process and stress

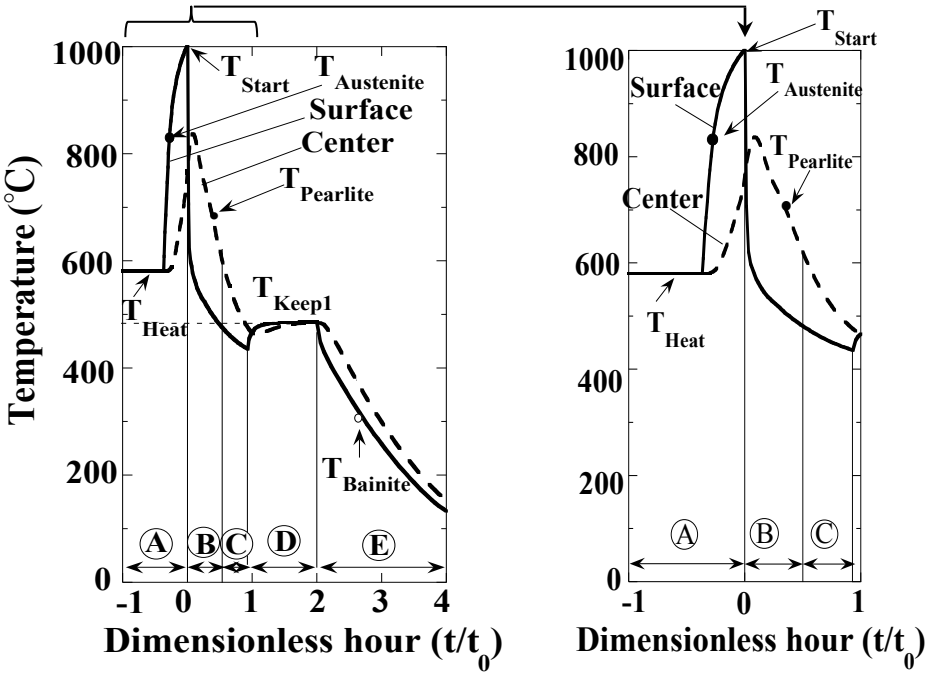

(a) Temperature histories at the center and surface

Ⓐ Rapid surface heating period
Ⓑ Rapid surface cooling period
Ⓒ Core material phase transformation period
Ⓓ Keeping temperature period
Ⓔ Air cooling and shell material phase transformation period

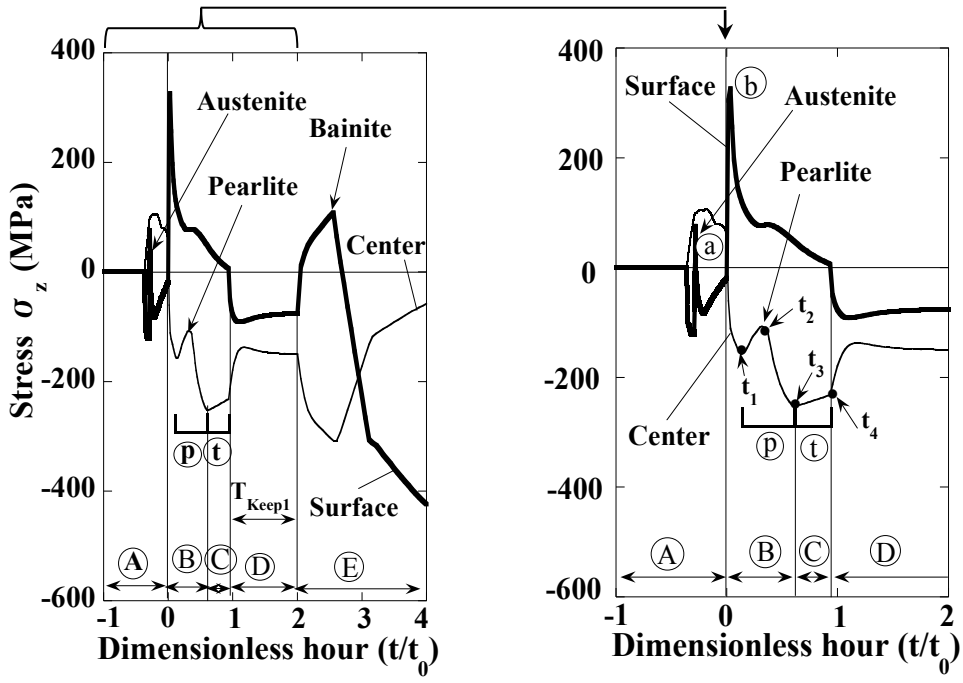

(b) Stress σ_z histories at the center and surface

ⓐ Austenite transformation
ⓑ Peak tensile residual stress at the surface

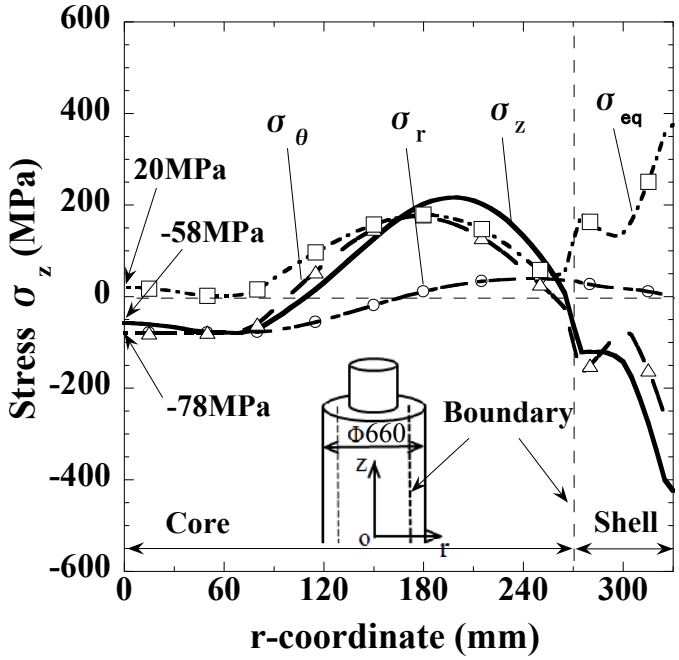

(c) Residual stress distribution form center to surface

Figure 4. Non-uniform heating process and stress

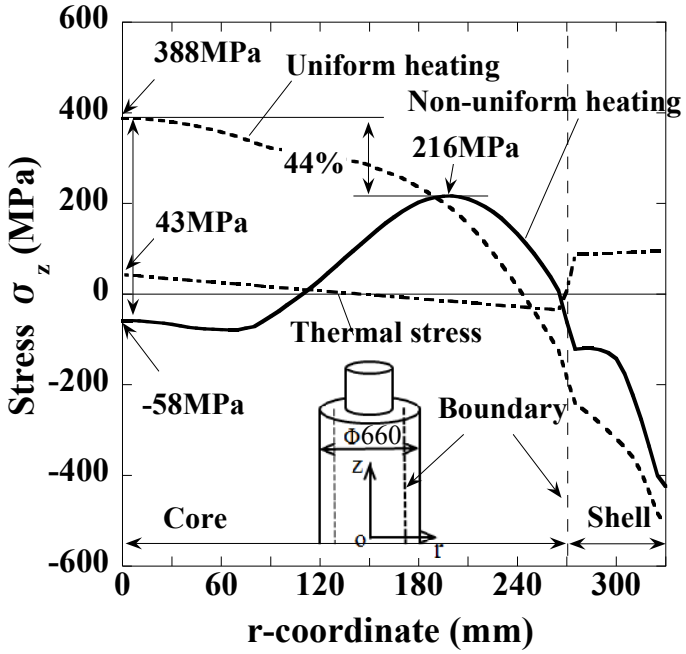

Figure 5. Comparison of residual stress distributions σ_z due to quenching after non-uniform and uniform heating

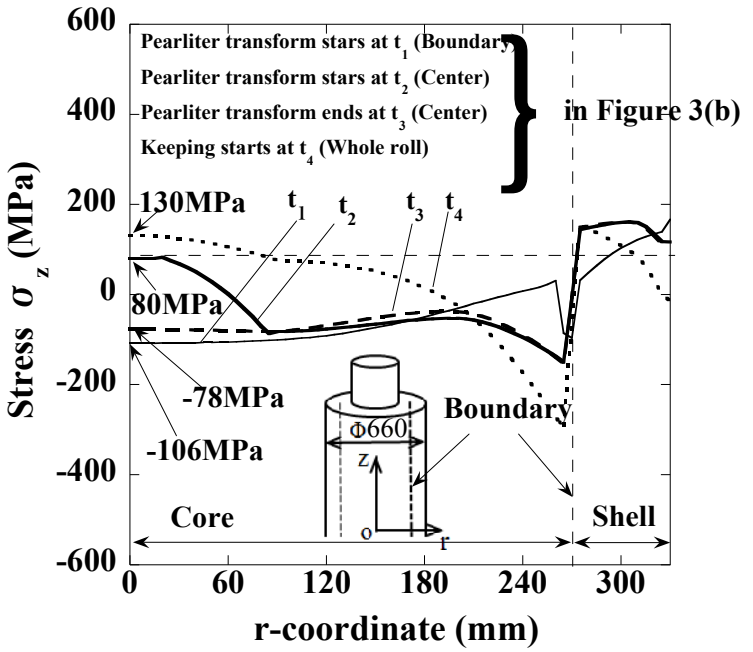

(a) Uniform heating and quenching

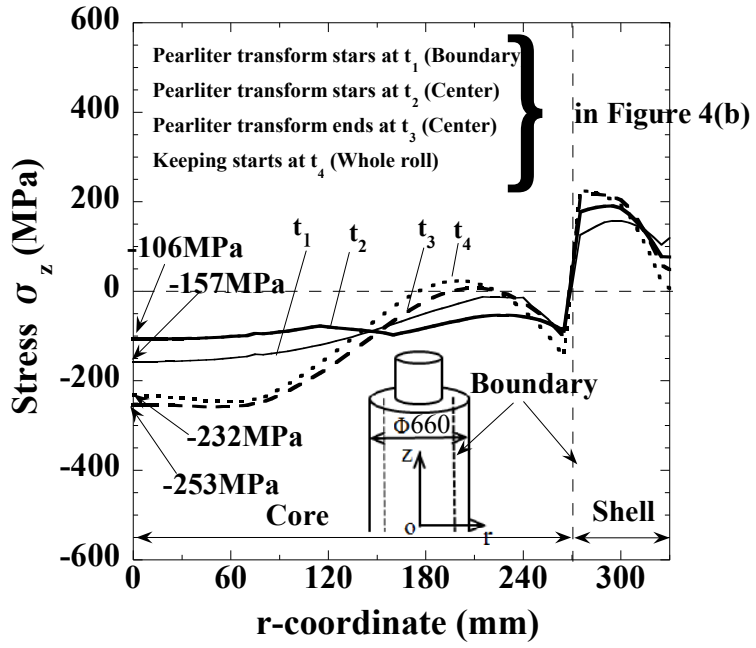

(b) Non-uniform heating and quenching

Figure 6. Stress distribution σ_z during Ⓑ and Ⓒ before keeping process (Time $t_1 \sim t_4$ is indicated in Figure 3(b) and Figure 4(b).)

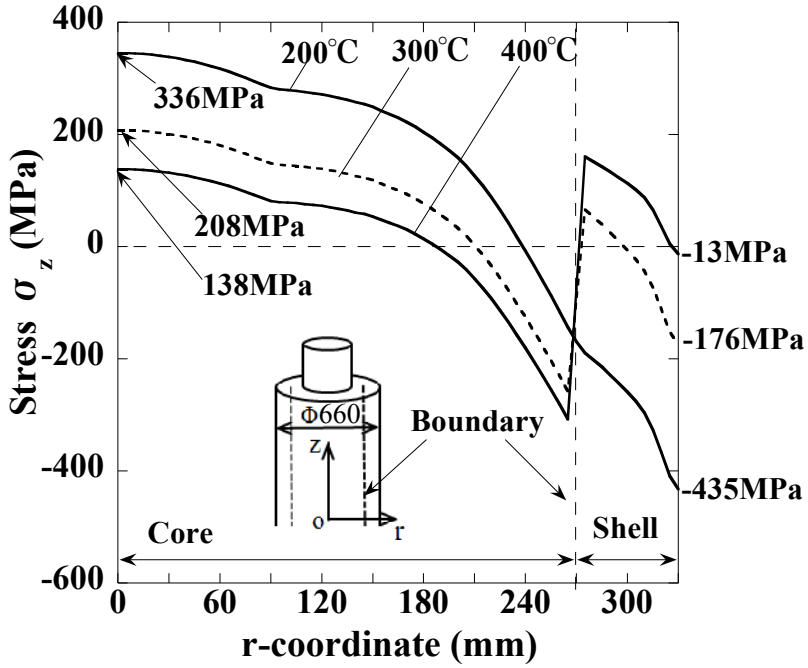

(a) Uniform heating and quenching

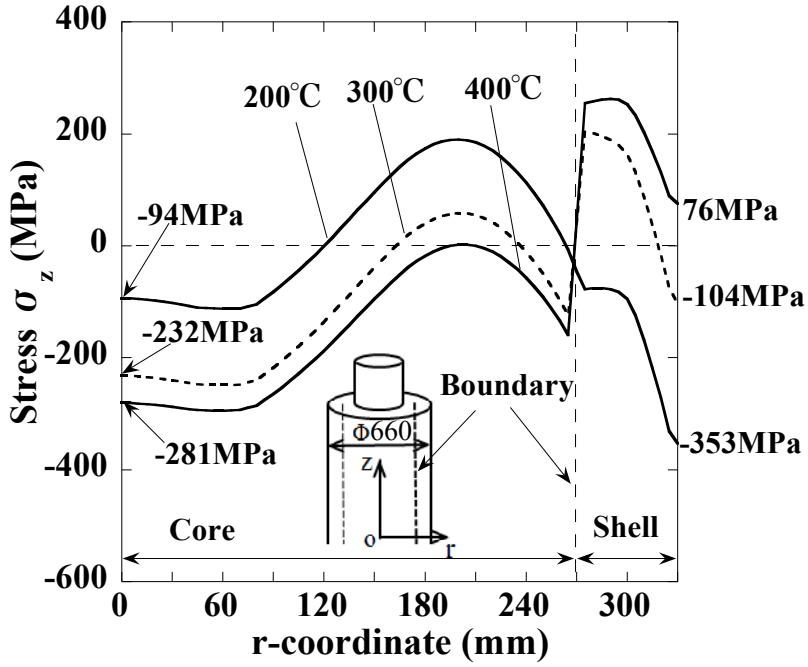

(b) Non-uniform heating and quenching

Figure 7 Stress distribution σ_z after keeping process when the surface temperature is 200℃, 300℃ and 400℃

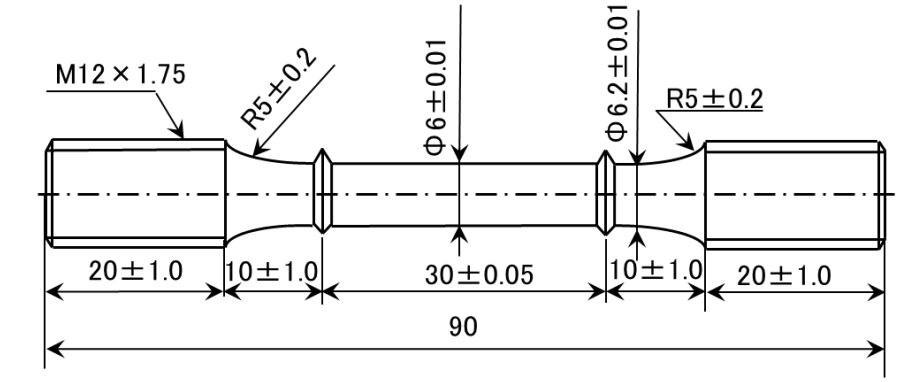

(a) Specimen of the creep test (mm)

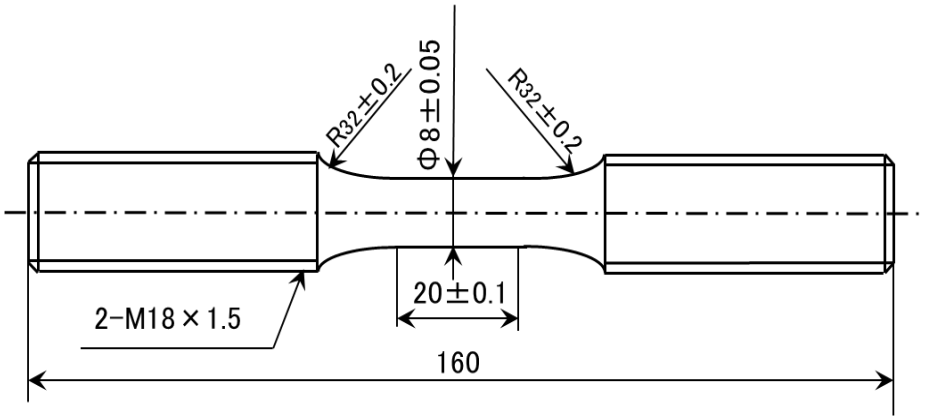

(b) Specimen of the stress relaxation test (mm)

Figure 8. Specimens of the creep test and stress relaxation test

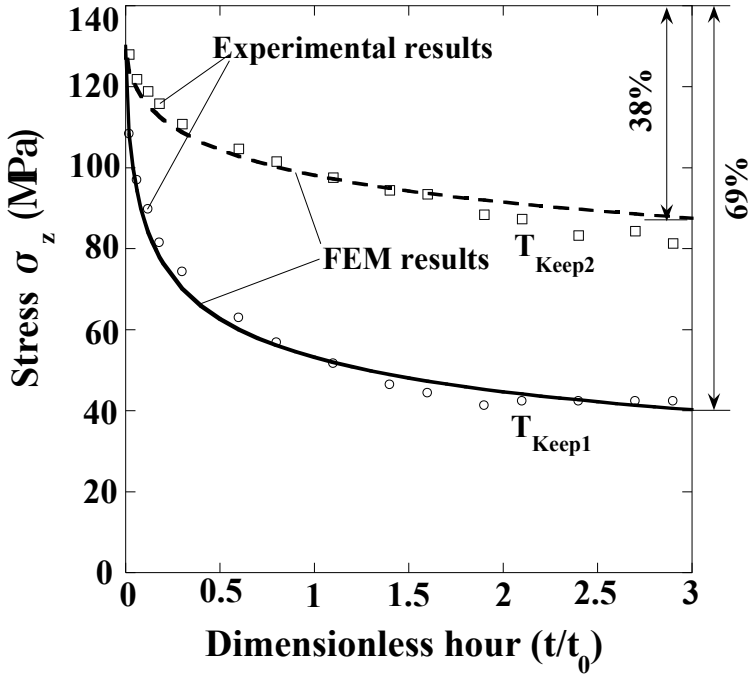

Figure 9. Comparison between FEM simulation results and experimental results for stress relaxation at T_{keep1} and T_{keep2}

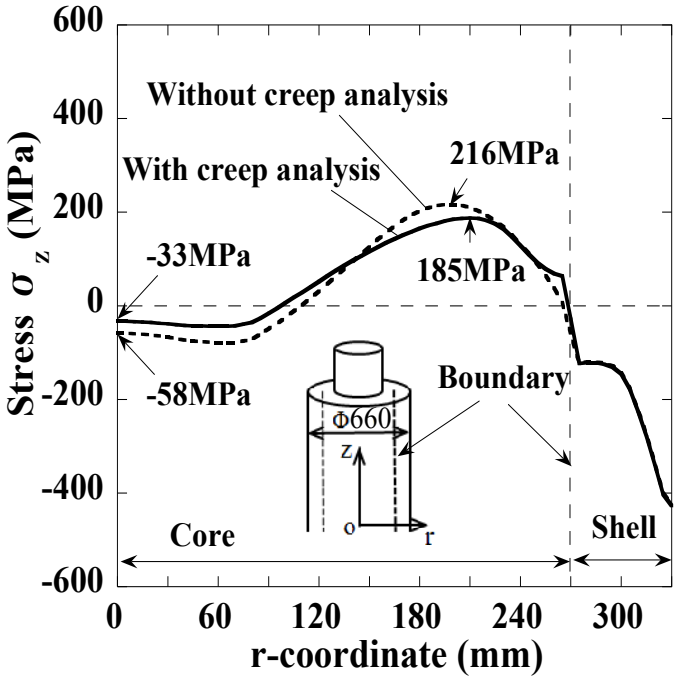

(a) Non-uniform heating quenching process

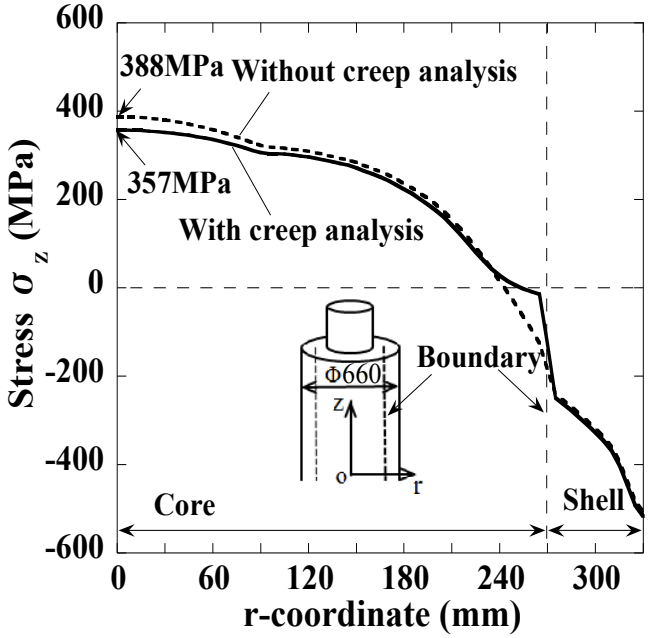

(b) Uniform heating quenching process

Figure 10. Effect of creep behavior on the residual stress

Table 1. Chemical compositions and mechanical properties of high speed steel and ductile casting iron for high speed steel roll

(a)Chemical compositions /mass%

Composition	C	Si	Mn	P	S	Ni
HSS	1~3	<2	<1.5			<5
DCI	2.5~4	1.5~3.1		<0.1	<0.1	0.4~5

Cr	Mo	Co	V	W	Mg
2~7	<10	<10	3~10	<20	<10
0.01~1.5	0.1~1				0.02~0.08

(b) Mechanical properties for high speed steel and ductile casting iron at room temperature

Property	HSS	DCI
0.2% proof stress [MPa]	(1282)[*1]	415
Young's modulus [GPa]	233	173
Poisson's ratio	0.3	0.3
Density [kg/m^3]	7.6	7.3
Thermal expansion coefficient [K^{-1}]	12.6×10-^{6}	13.0×10^{-6}
Thermal conductivity [W/(m・K)]	20.2	23.4
Specific heat [J/(kg・K)]	0.46	0.46

[1)] Tensile strength of the shell material is indicated as the 0.2% proof stress because the deformation at break is small

Table 2. Comparison of keeping process between non-uniform heating quenching and uniform heating quenching

Heat treatment	Non-uniform	Uniform
Stress relaxation ratio (%)	69	38
Keeping temperature (℃)	$T_{Keep1} > T_{Keep2}$	
σ_{eq} at keeping temperature(MPa)	136	103
Keeping time (h)	5.3	6